Fermi National Accelerator Laboratory

FERMILAB-Pub-93/032-E
CDF

The Center-of-Mass Angular Distribution of Prompt Photons Produced in $p\bar{p}$ Collisions at $\sqrt{s}$ = 1.8 TeV

F. Abe et al
The CDF Collaboration

Fermi National Accelerator Laboratory
P.O. Box 500, Batavia, Illinois 60510

March 1993

Submitted to *Physical Review Letters*

Operated by Universities Research Association Inc. under Contract No. DE-AC02-76CHO3000 with the United States Department of Energy

Disclaimer

This report was prepared as an account of work sponsored by an agency of the United States Government. Neither the United States Government nor any agency thereof, nor any of their employees, makes any warranty, express or implied, or assumes any legal liability or responsibility for the accuracy, completeness, or usefulness of any information, apparatus, product, or process disclosed, or represents that its use would not infringe privately owned rights. Reference herein to any specific commercial product, process, or service by trade name, trademark, manufacturer, or otherwise, does not necessarily constitute or imply its endorsement, recommendation, or favoring by the United States Government or any agency thereof. The views and opinions of authors expressed herein do not necessarily state or reflect those of the United States Government or any agency thereof.

CDF/PUB/JET/PUBLIC 1915
Fermilab-Pub-93/032-E

The Center-of-Mass Angular Distribution of Prompt Photons Produced in $p\bar{p}$ Collisions at $\sqrt{s} = 1.8$ TeV

F. Abe,[12] M. Albrow,[6] D. Amidei,[15] C. Anway-Wiese,[3] G. Apollinari,[23] M. Atac,[6] P. Auchincloss,[22] P. Azzi,[17] A. R. Baden,[8] N. Bacchetta,[16] W. Badgett,[15] M. W. Bailey,[21] A. Bamberger,[6,a] P. de Barbaro,[22] A. Barbaro-Galtieri,[13] V. E. Barnes,[21] B. A. Barnett,[11] G. Bauer,[14] T. Baumann,[8] F. Bedeschi,[20] S. Behrends,[2] S. Belforte,[20] G. Bellettini,[20] J. Bellinger,[28] D. Benjamin,[27] J. Benlloch,[14] J. Bensinger,[2] A. Beretvas,[6] J. P. Berge,[6] S. Bertolucci,[7] K. Biery,[10] S. Bhadra,[9] M. Binkley,[6] D. Bisello,[17] R. Blair,[1] C. Blocker,[2] A. Bodek,[22] V. Bolognesi,[20] A. W. Booth,[6] C. Boswell,[11] G. Brandenburg,[8] D. Brown,[8] E. Buckley-Geer,[6] H. S. Budd,[22] G. Busetto,[17] A. Byon-Wagner,[6] K. L. Byrum,[1] C. Campagnari,[6] M. Campbell,[15] A. Caner,[6] R. Carey,[8] W. Carithers,[13] D. Carlsmith,[28] J. T. Carroll,[6] R. Cashmore,[6,a] A. Castro,[17] Y. Cen,[18] F. Cervelli,[20] K. Chadwick,[6] J. Chapman,[15] G. Chiarelli,[7] W. Chinowsky,[13] S. Cihangir,[6] A. G. Clark,[6] M. Cobal,[20] D. Connor,[18] M. Contreras,[4] J. Cooper,[6] M. Cordelli,[7] D. Crane,[6] J. D. Cunningham,[2] C. Day,[6] F. DeJongh,[6] S. Dell'Agnello,[20] M. Dell'Orso,[20] L. Demortier,[23] B. Denby,[6] P. F. Derwent,[15] T. Devlin,[24] D. DiBitonto,[25] M. Dickson,[22] R. B. Drucker,[13] K. Einsweiler,[13] J. E. Elias,[6] R. Ely,[13] S. Eno,[4] S. Errede,[9] A. Etchegoyen,[6,a] B. Farhat,[14] M. Frautschi,[16] G. J. Feldman,[8] B. Flaugher,[6] G. W. Foster,[6] M. Franklin,[8] J. Freeman,[6] H. Frisch,[4] T. Fuess,[6] Y. Fukui,[12] A. F. Garfinkel,[21] A. Gauthier,[9] S. Geer,[6] D. W. Gerdes,[15] P. Giannetti,[20] N. Giokaris,[23] P. Giromini,[7] L. Gladney,[18] M. Gold,[16] J. Gonzalez,[18] K. Goulianos,[23] H. Grassmann,[17] G. M. Grieco,[20] R. Grindley,[10] C. Grosso-Pilcher,[4] C. Haber,[13] S. R. Hahn,[6] R. Handler,[28] K. Hara,[26] B. Harral,[18] R. M. Harris,[6] S. A. Hauger,[5] J. Hauser,[3] C. Hawk,[24] T. Hessing,[25] R. Hollebeek,[18] L. Holloway,[9] A. Hölscher,[10] S. Hong,[15] G. Houk,[18] P. Hu,[19] B. Hubbard,[13] B. T. Huffman,[19] R. Hughes,[22] P. Hurst,[8] J. Huth,[6] J. Hylen,[6] M. Incagli,[20] T. Ino,[26] H. Iso,[26] H. Jensen,[6] C. P. Jessop,[8] R. P. Johnson,[6] U. Joshi,[6] R. W. Kadel,[13] T. Kamon,[25] S. Kanda,[26] D. A. Kardelis,[9] I. Karliner,[9] E. Kearns,[8] L. Keeble,[25] R. Kephart,[6] P. Kesten,[2] R. M. Keup,[9] H. Keutelian,[6] D. Kim,[6] S. B. Kim,[15] S. H. Kim,[26] Y. K. Kim,[13] L. Kirsch,[2] K. Kondo,[26] J. Konigsberg,[8] K. Kordas,[10] E. Kovacs,[6] M. Krasberg,[15] S. E. Kuhlmann,[1] E. Kuns,[24] A. T. Laasanen,[21] S. Lammel,[3] J. I. Lamoureux,[28] S. Leone,[20] J. D. Lewis,[6] W. Li,[1] P. Limon,[6] M. Lindgren,[3] T. M. Liss,[9] N. Lockyer,[18] M. Loreti,[17] E. H. Low,[18] D. Lucchesi,[20] C. B. Luchini,[9] P. Lukens,[6] P. Maas,[28] K. Maeshima,[6] M. Mangano,[20] J. P. Marriner,[6] M. Mariotti,[20] R. Markeloff,[28] L. A. Markosky,[28] J. Matthews,[16] R. Mattingly,[2]

Submitted to Physical Review Letters March 1, 1993

P. McIntyre,[25] A. Menzione,[20] E. Meschi,[20] T. Meyer,[25] S. Mikamo,[12] M. Miller,[4] T. Mimashi,[26] S. Miscetti,[7] M. Mishina,[12] S. Miyashita,[26] Y. Morita,[26] S. Moulding,[23] J. Mueller,[24] A. Mukherjee,[6] T. Muller,[3] L. F. Nakae,[2] I. Nakano,[26] C. Nelson,[6] D. Neuberger,[3] C. Newman-Holmes,[6] J. S. T. Ng,[8] M. Ninomiya,[26] L. Nodulman,[1] S. Ogawa,[26] R. Paoletti,[20] V. Papadimitriou,[6] A. Para,[6] E. Pare,[8] S. Park,[6] J. Patrick,[6] G. Pauletta,[20] L. Pescara,[17] G. Piacentino,[20] T. J. Phillips,[5] F. Ptohos,[8] R. Plunkett,[6] L. Pondrom,[28] J. Proudfoot,[1] G. Punzi,[20] D. Quarrie,[6] K. Ragan,[10] G. Redlinger,[4] J. Rhoades,[28] M. Roach,[27] F. Rimondi,[6,a] L. Ristori,[20] W. J. Robertson,[5] T. Rodrigo,[6] T. Rohaly,[18] A. Roodman,[4] W. K. Sakumoto,[22] A. Sansoni,[7] R. D. Sard,[9] A. Savoy-Navarro,[6] V. Scarpine,[9] P. Schlabach,[8], E. E. Schmidt,[6] O. Schneider,[13] M. H. Schub,[21] R. Schwitters,[8] G. Sciacca,[20] A. Scribano,[20] S. Segler,[6] S. Seidel,[16] Y. Seiya,[26] G. Sganos,[10] M. Shapiro,[13] N. M. Shaw,[21] M. Sheaff,[28] M. Shochet,[4] J. Siegrist,[13] A. Sill,[22] P. Sinervo,[10] J. Skarha,[11] K. Sliwa,[27] D. A. Smith,[20] F. D. Snider,[11] L. Song,[6] T. Song,[15] M. Spahn,[13] A. Spies,[11] P. Sphicas,[14] R. St. Denis,[8] L. Stanco,[6,a] A. Stefanini,[20] G. Sullivan,[4] K. Sumorok,[14] R. L. Swartz, Jr.,[9] M. Takano,[26] K. Takikawa,[26] S. Tarem,[2] F. Tartarelli,[20] S. Tether,[14] D. Theriot,[6] M. Timko,[27] P. Tipton,[22] S. Tkaczyk,[6] A. Tollestrup,[6] J. Tonnison,[21] W. Trischuk,[8] Y. Tsay,[4] J. Tseng,[11] N. Turini,[20] F. Ukegawa,[26] D. Underwood,[1] S. Vejcik, III,[15] R. Vidal,[6] R. G. Wagner,[1] R. L. Wagner,[6] N. Wainer,[6] R. C. Walker,[22] J. Walsh,[18] G. Watts,[22] T. Watts,[24] R. Webb,[25] C. Wendt,[28] H. Wenzel,[20] W. C. Wester, III,[13] T. Westhusing,[9] S. N. White,[23] A. B. Wicklund,[1] E. Wicklund,[6] H. H. Williams,[18] B. L. Winer,[22] J. Wolinski,[25] D. Y. Wu,[15] X. Wu,[20] J. Wyss,[17] A. Yagil,[6] K. Yasuoka,[26] Y. Ye,[10] G. P. Yeh,[6] J. Yoh,[6] M. Yokoyama,[26] J. C. Yun,[6] A. Zanetti,[20] F. Zetti,[20] S. Zhang,[15] W. Zhang,[18] S. Zucchelli,[6,a]

The CDF Collaboration

[1] *Argonne National Laboratory, Argonne, Illinois 60439*

[2] *Brandeis University, Waltham, Massachusetts 02254*

[3] *University of California at Los Angeles, Los Angeles, California 90024*

[4] *University of Chicago, Chicago, Illinois 60637*

[5] *Duke University, Durham, North Carolina 27706*

[6] *Fermi National Accelerator Laboratory, Batavia, Illinois 60510*

[7] *Laboratori Nazionali di Frascati, Istituto Nazionale di Fisica Nucleare, Frascati, Italy*

[8] *Harvard University, Cambridge, Massachusetts 02138*

[9] *University of Illinois, Urbana, Illinois 61801*

[10] *Institute of Particle Physics, McGill University, Montreal, and University of Toronto, Toronto, Canada*

[11] *The Johns Hopkins University, Baltimore, Maryland 21218*

[12] *National Laboratory for High Energy Physics (KEK), Japan*

(13) *Lawrence Berkeley Laboratory, Berkeley, California 94720*
(14) *Massachusetts Institute of Technology, Cambridge, Massachusetts 02139*
(15) *University of Michigan, Ann Arbor, Michigan 48109*
(16) *University of New Mexico, Albuquerque, New Mexico 87131*
(17) *Universita di Padova, Instituto Nazionale di Fisica Nucleare, Sezione di Padova, I-35131 Padova, Italy*
(18) *University of Pennsylvania, Philadelphia, Pennsylvania 19104*
(19) *University of Pittsburgh, Pittsburgh, Pennsylvania 15260*
(20) *Istituto Nazionale di Fisica Nucleare, University and Scuola Normale Superiore of Pisa, I-56100 Pisa, Italy*
(21) *Purdue University, West Lafayette, Indiana 47907*
(22) *University of Rochester, Rochester, New York 15627*
(23) *Rockefeller University, New York, New York 10021*
(24) *Rutgers University, Piscataway, New Jersey 08854*
(25) *Texas A&M University, College Station, Texas 77843*
(26) *University of Tsukuba, Tsukuba, Ibaraki 305, Japan*
(27) *Tufts University, Medford, Massachusetts 02155*
(28) *University of Wisconsin, Madison, Wisconsin 53706*

Abstract

Data taken with the Collider Detector at Fermilab (CDF) during the 1988-1989 run of the Tevatron are used to measure the center-of-mass angular distribution between isolated prompt photons and the beam direction. The shape of the angular distribution for photon-jet events is found to be significantly different from that observed in dijet data. The next to leading order (NLO) QCD predictions show qualitative agreement with the observed prompt photon angular distribution.

PACS Numbers: 12.38.QK, 13.85.Qk, 14.80.Er

Prompt photons produced in $p\bar{p}$ collisions provide good quantitative tests of perturbative Quantum Chromodynamics (QCD). Previous publications from UA2 [1] and CDF [2] have shown good agreement between data and the predicted prompt photon cross section over a wide range of photon and center-of-mass (CM) energies. Perturbative QCD predicts that the CM angular distribution of prompt photon events will differ significantly from that of dijet events. The UA2 collaboration demonstrated this by plotting the ratio of the photon/dijet CM angular distributions [3]. Leading order (LO) prompt photon production, at Tevatron energies, is dominated by the t-channel quark exchange process ($gq \rightarrow q\gamma$); here the spin $\frac{1}{2}$ quark propagator produces a photon angular distribution roughly of the form $(1-\cos\theta^*)^{-1}$, where θ^* is the CM polar angle. In contrast, dijet production is dominated by the t-channel gluon exchange process ($gg \rightarrow gg$), where the spin 1 gluon produces a jet angular distribution roughly of the form $(1-\cos\theta^*)^{-2}$. Here we present the first measurement of the

prompt photon CM angular distribution at $\sqrt{s}$=1.8 TeV and compare it to LO and NLO QCD. The data sample corresponds to an integrated luminosity of 3.3 pb^{-1} [4].

CDF has been described in detail elsewhere [5]. We describe here briefly those detector subsystems used in this analysis. We use a coordinate system defined such that z is along the proton beam direction, ϕ is the azimuthal angle and θ the polar angle. The central region ($|\eta| < 1.1$, where η is the pseudorapidity) contains a 1.4 Tesla superconducting solenoid enclosing the vertex time projection chamber and the central tracking chamber. Outside the coil are situated the central electromagnetic (CEM) and hadronic calorimeters consisting of lead-scintillator and steel-scintillator sandwiches respectively. Imbedded within the CEM are the central electromagnetic strip chambers (CES) whose finer segmentation allow the measurement of the lateral shower profiles in ϕ and z views. The area outside the central region ($1.1 < |\eta| < 4.2$) is instrumented with gas calorimeters divided into electromagnetic (lead absorber) and hadronic (steel absorber) compartments.

The data satisfied a trigger requiring an isolated electromagnetic cluster with a minimum transverse energy ($E_T = E \sin\theta$) of 23 GeV in the CEM [4]. The candidate events were reconstructed and energy corrections were applied to the EM and jet clusters [4] [6]. Additional requirements were imposed to ensure that photons were well measured. These include a cut on the pseudorapidity of the photon ($|\eta_\gamma| < 0.9$), a maximum displacement along z of the event vertex from the center of the detector ($|z_{vert}| < 50$ cm) and fiducial cuts to avoid dead regions of the detector.

Stringent isolation requirements were placed upon the photon candidates. The photon candidate cluster was required to have no secondary strip (CES) clusters of E_T >1.0 GeV and have less than 2.0 GeV unclustered EM E_T (CEM) within a cone radius R=0.7, where R=$\sqrt{\Delta\phi^2 + \Delta\eta^2}$.

The stringent isolation cuts and a veto on any tracks pointing to the calorimeter tower of the photon candidate reduce the possible prompt photon backgrounds to events where a QCD jet fragments into a single isolated neutral meson that decays into *multiple* photons. While jet fragmentation into single isolated particles is rare, the inclusive jet cross section [6] is approximately three orders of magnitude higher than the prompt photon cross section [2] at similar energies. As a result, the absolute background and signal production probabilities are roughly comparable after the application of isolation cuts. The final data sample was about 65% signal and 35% background.

The background subtraction method exploits the average difference in shower profiles expected from events with single isolated prompt photons and those with multiple photons originating from decaying neutral mesons. The shower profiles in both ϕ and z views are compared to a sample profile obtained from test beam electrons and a χ^2 is extracted for each view on an event by event basis. The average ($\chi^2_{\rm ave}$) of the two views is then used for the background subtraction. A simulation was run to determine the expected $\chi^2_{\rm ave}$ distributions as a function of p_T for signal and an expected background mix of π^0's, η's and K^0_s's. The details of the simulation and the

determination of the likely background mix can be found in [4]. The $\chi^2_{\rm ave}$ distributions from the simulation are then reduced to a p_T dependent efficiency for both the signal and the background. These efficiencies are used to calculate signal and background weights (which sum to 1) for an individual event. The sum of the signal weights for all events passing the cuts is the background subtracted result. The method breaks down when a pair of photons from a decaying π^0 are sufficiently boosted to the point where their angular separation is less than the resolution of the strip chambers. Therefore a maximum p_T cut of 45 GeV/c is imposed.

In an effort to retain the simplicity of the $2 \rightarrow 2$ system, we vectorially sum the momentum from jets opposite to the photon, in ϕ, to create a single 'summed' jet. We require that the highest p_T jet be in the opposite hemisphere in ϕ from the photon and that the jet p_T be > 10 GeV/c after all energy corrections. The CM variables are found from the p_T and direction of the photon candidate and the direction of the summed jet. We then add in second or third jets if they are also in the opposite hemisphere and have a corrected $p_T > 10$ GeV/c.

The angular distribution presented is $\frac{{\rm d}^2N}{{\rm dp}^*{\rm dcos}\theta^*}$, where we have integrated over a range of the CM momentum p^*. Since there can be no angular asymmetry in this measurement, we plot $\mid \cos\theta^* \mid$. In the case of a $2 \rightarrow 2$ system, the CM variables p^*, η^* and $\eta_{\rm Boost}$ can be found from the p_T of the photon, and the detector positions of the photon and the jet (η_γ, $\eta_{\rm Jet}$) *via*: $\eta^* = \frac{\eta_\gamma - \eta_{\rm Jet}}{2}$, $\eta_{\rm Boost} = \frac{\eta_\gamma + \eta_{\rm Jet}}{2}$, $p^* = p_T \cosh\eta^*$ and $\cos\theta^* = \tanh\eta^*$.

Var	Region 1	Region 2
$\pm\cos\theta^*$	0.0 to $\pm$0.6	$\pm$0.3 to $\pm$0.8
$\pm\eta^*$	0.0 to $\pm$0.7	$\pm$0.3 to $\pm$1.1
$\eta_{\rm Boost}$	$\mp$0.9 to $\pm$0.2	$\mp$1.2 to $\mp$0.2
p^*	27.8 to 45.0 GeV/c	36.7 to 47.0 GeV/c

Table 1: Table of cuts on the CM variables that ensure uniform acceptance for $\cos\theta^*$.

It is desirable to push the measurement to as large a value of $\cos\theta^*$ as possible because the differences between the theoretical calculations are most pronounced at small angles. Fig. 1 shows η_γ vs. $\eta_{\rm Jet}$ for the data on the horizontal-vertical axes; the diagonal axes are the transformation to η^* vs. $\eta_{\rm Boost}$. The limits on the η_γ acceptance implies that an $\eta^* = 0.9$ is the maximum value that could be measured in one uniform region of acceptance; this corresponds to $\cos\theta^* \sim 0.7$. In order to utilize as much of the data as possible, we select two regions (see Table 1), each uniform in η^* and $\eta_{\rm Boost}$ acceptance, and normalize in a region of overlap. The boxes in Fig. 1 define the regions of uniform acceptance in η^* and $\eta_{\rm Boost}$. The corresponding cuts for $\cos\theta^*$ are given in Table 1. The p^* limits for uniform acceptance are the result of the combined limits on p_T ($22 < p_T < 45$ GeV/c) and η^* (explicitly, $p^*_{\rm min} = p_{T\rm min} \cdot \cosh\eta^*_{\rm max}$ and $p^*_{\rm max} = p_{T\rm max} \cdot \cosh\eta^*_{\rm min}$). Fig. 2 plots p_T vs. η^* and illustrates this effect on the transformation to p^*.

The largest systematic uncertainty of the measurement comes from the statistics of the overlap region and therefore an increase in momentum bandwidth is vital to the measurement. Since the minimum p^* is determined in large part by the minimum p_T, we choose to lower the minimum p_T to 22 GeV/c, one GeV/c below the trigger

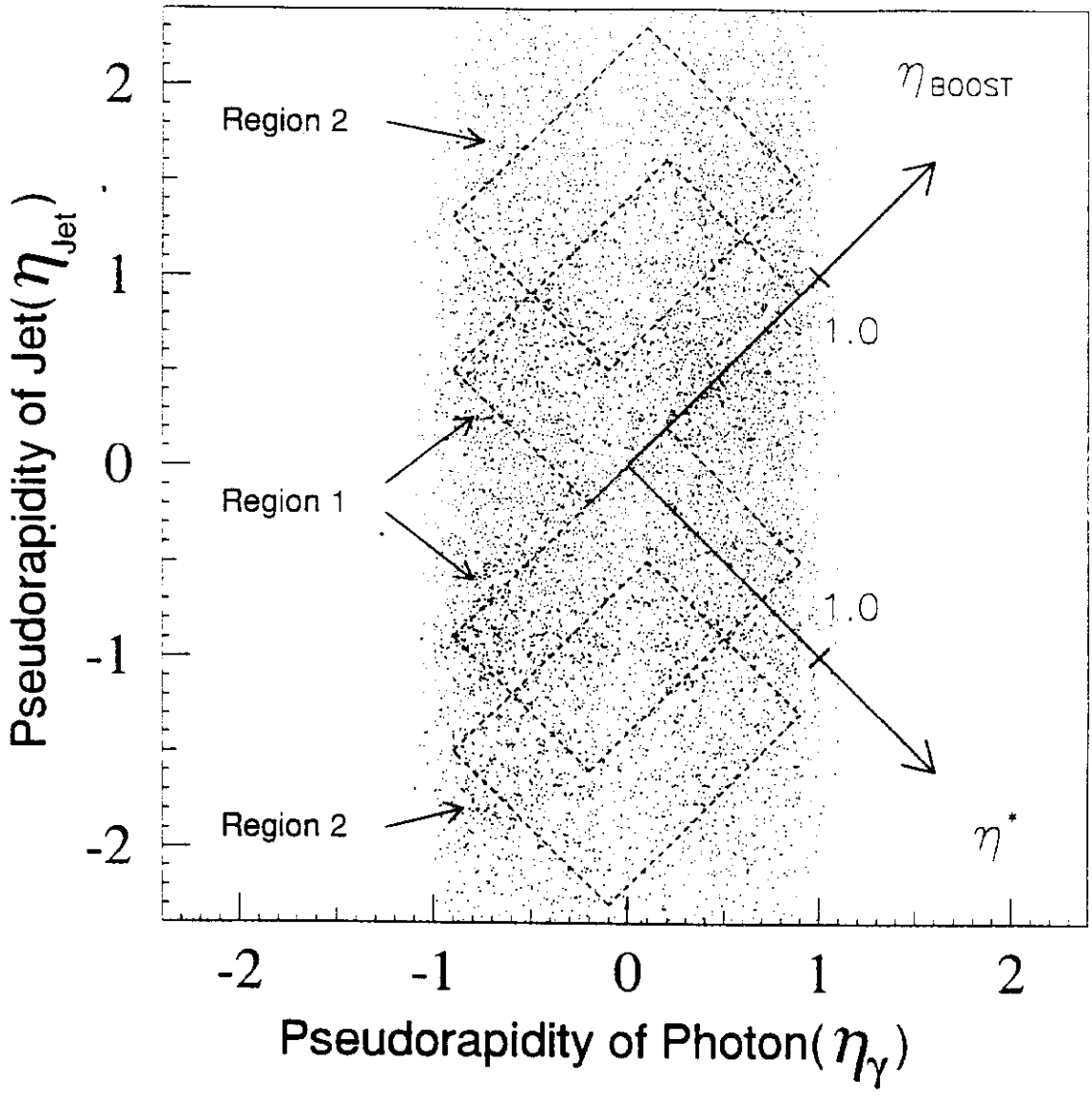

Figure 1: Data plotted $\eta_{\rm Jet}$ vs. η_γ. The diagonal axes are the sum ($\eta_{\rm Boost}$) and difference (η^*) axes. The overlapping regions are used for normalization.

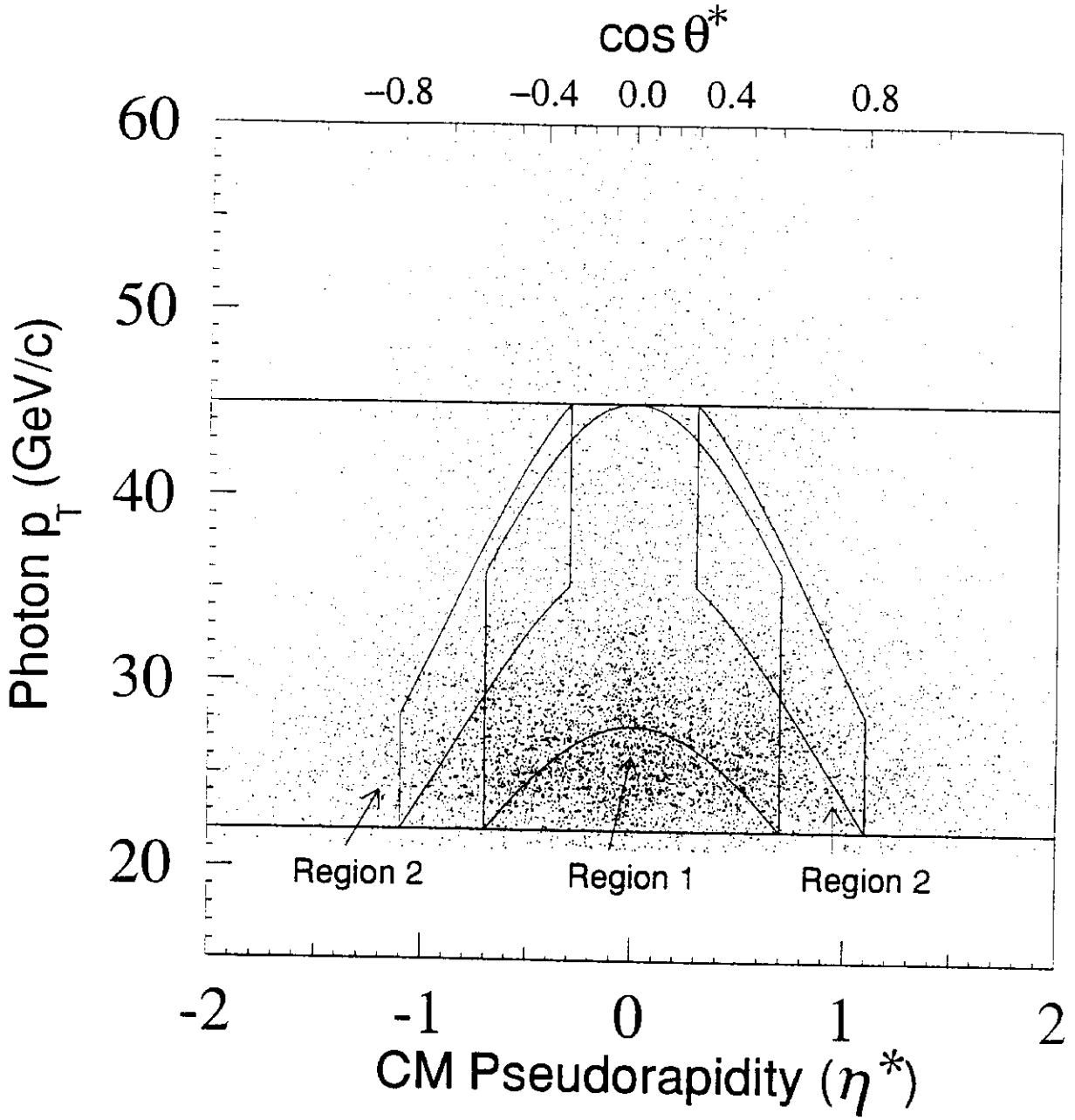

Figure 2: Data plotted p_T vs. η^*. The vertical lines delineate the regions in η^* ($\cosh\theta^*$) and the curves are contours of constant p^*. The points within the curves are regions of flat acceptance in p^* and η^*. The horizontal lines are the upper and lower limits of $p_{T\min} = 22$ GeV/c and $p_{T\max} = 45$ GeV/c which along with the limits on η^* correspond to $27.6 < p^* < 45.0$ GeV/c and $36.7 < p^* < 47.0$ GeV/c in each of the uniform acceptance regions. The $\cos\theta^*$ scale is given along the upper axis for reference.

threshold and correct for trigger inefficiencies where appropriate. The events with low p_T ($22 < p_T < 24$) have large efficiency uncertainties ($\sim 20\%$), but they occur only in the last bin of high $\cos\theta^*$ in each region, where they contribute only a small fraction of the total signal ($< 8\%$). However, lowering the minimum p_T gives us a band of increased p^* acceptance over the full range of $\cos\theta^*$ which substantially reduces the normalization uncertainty (see Fig. 2). The trigger efficiency for the data sample was measured through the use of a lower threshold trigger. No η^* trigger dependence was found [7]. The photon candidates with p_T's below threshold come from events whose trigger cluster was above 23 GeV/c but had their energy corrected to a lower p_T.

Fig. 3 shows the prompt photon $\cos\theta^*$ distribution after background subtraction plotted against predictions from a full NLO [8] and a LO tree-level diagram calculation [9] of prompt photon production. Also shown are a LO calculation [9] of dijet production and dijet data from CDF [10]. The inner error bars of Fig. 3 show the statistical uncertainties only, the outer are the statistical and systematic uncertainties added in quadrature. The prompt photon data show rough agreement with both LO and NLO theory but do not agree with dijet data or theory. The theory curves were generated at the parton level and were required to pass the same isolation requirements as the data. In the NLO calculations the outgoing partons were summed and the resultant direction was used to calculate $\cos\theta^*$, in the same fashion as the data. All theory curves and data have a normalization such that the flat part of the curve $|\cos\theta^*| < 0.3$ has an area of 0.3. The unnormalized (N_γ) and normalized

$\lvert\cos\theta^*\rvert$	N_γ	Stat Err	Sys Err	N_γ^{Norm}
0.0-0.1	147.9	±28.2	±22.7	1.086
0.1-0.2	131.2	29.4	17.3	0.964
0.2-0.3	129.2	28.1	16.8	0.949
0.3-0.4	124.6	27.6	16.9	0.915
0.4-0.5	129.0	32.6	26.9	0.947
0.5-0.6	250.2	43.7	39.8	1.838
0.6-0.7	95.6	20.7	26.1	2.782
0.7-0.8	164.6	33.5	46.1	4.790

Table 2: Table of the background subtracted data and uncertainties. N_γ are the unnormalized data and N_γ^{Norm} are the normalized data as shown in Fig. 3.

(N_γ^{Norm}) background subtracted data are presented in Table 2 along with the unnormalized statistical and systematic uncertainties. The unnormalized data are the number of photon events found in each bin of $\cos\theta^*$ after background subtraction, trigger efficiency and acceptance corrections.

The systematic uncertainties include effects from the normalization, uncertainties in the χ^2's distributions for background subtraction, trigger efficiency and acceptance [7]. The normalization uncertainty was estimated with the 1σ statistical variation within the regions used for normalization. This was found to be the dominant uncertainty and is completely correlated between the first six points (~12%) and between the last two (~27%). The uncertainties on the angular distribution due to the background subtraction and trigger efficiency uncertainty were found by repeating the analysis with the simulation χ^2_{ave} distributions and trigger efficiency varied independently by their 1 σ uncertainties. Both uncertainties get larger with increasing $\cos\theta^*$ reaching a maximum of 14% and 7% respectively. The systematic uncertainties from η^* and η_{Boost} acceptance were found from a MC detector simulation to be $< 5\%$ [7].

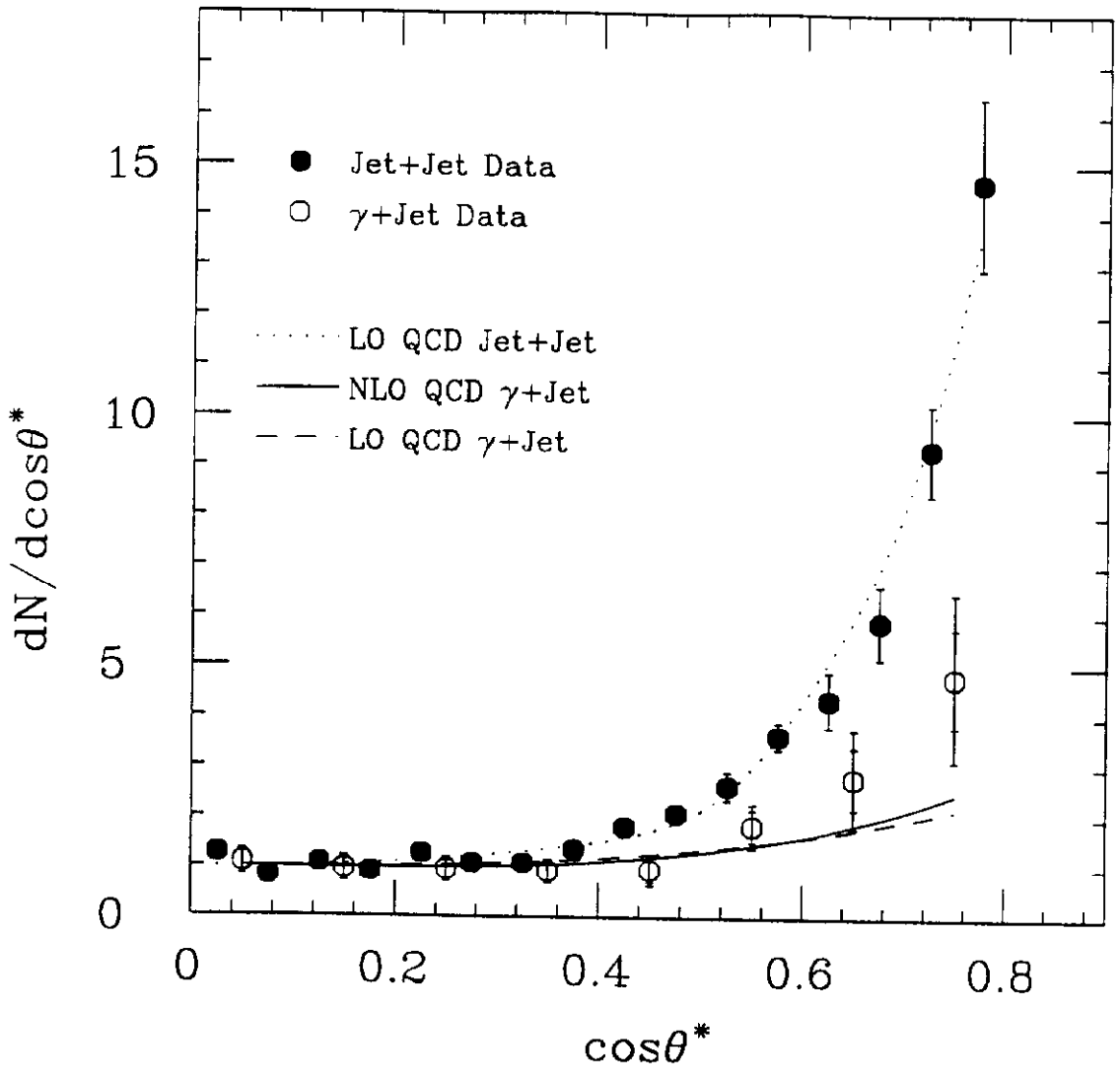

Figure 3: Prompt photon dN/dcos θ^* after background subtraction. The photon data (open circles) are compared to LO-QCD (dashes) and NLO-QCD (solid) [8]. Also shown are previously published dijet data [10] (solid circles) and theory curves for LO dijet tree level diagrams [9] (dots). The data and theory curves are normalized to an area of 3.0 in the region $|\cos\theta^*| < 0.3$.

In conclusion, we find the prompt photon CM angular distribution to be significantly different from the corresponding dijet angular distribution. The data are also found to agree with NLO QCD with a confidence level of 52% for prompt photon production. Note that the normalization for the last two points is 100% correlated and has the largest systematic uncertainty. When only the statistical errors are used, the confidence level with NLO QCD is 7%. While the effects of photon *bremsstrahlung* are accounted for at some level in the present NLO calculations, the presence of a larger *bremsstrahlung* component in the data would tend to create an excess at high $\cos\theta^*$.

The authors wish to thank the technical and support staffs of Fermilab and the participating institutions. We would also like to thank B. Baily, J.F. Owens and J. Ohnemus for use of the results of their theoretical calculations. This work was supported by the U.S. Department of Energy and National Science Foundation, the Italiano Istituto Nazionale di Fisica Nucleare, the Ministry of Science, Culture and Education of Japan, the Natural Sciences and the Alfred P. Sloan Foundation.

References

[a]Visitor

[1] UA2 Collaboration, J. Alitti *et al*, Phys. Lett. B **263**, 544 (1991).

[2] F. Abe *et al*, Phys. Rev. Lett. **68**, 2734 (1992).

[3] UA2 Collaboration, J. Alitti *et al*, Phys. Lett. B **288**. 386 (1992).

[4] R. Harris *et al*, Fermilab-PUB-92/01-E, 1992 (to be published in Phys. Rev. D.).

[5] F. Abe *et al*, Nucl. Instrum. Methods Phys. Res., Sect. A **271**, 387 (1988).

[6] F. Abe *et al*, Phys. Rev. Lett. **68**, 1104 (1992).

[7] L. Nakae, Ph.D. thesis, Brandeis University, April 1992.

[8] H. Bauer, J. Ohnemus and J.F. Owens, Phys. Lett. **234B**, 127 (1990).

[9] I Hinchcliffe, Papageno Event Generator, Private Communication.

[10] F. Abe *et al*, Phys. Rev. Lett. **62**, 3020 (1989).